Measurements of Higgs boson production in decays to two tau leptons with the ATLAS detector

Michaela Mlynáriková (Northern Illinois University)
on behalf of the ATLAS collaboration

EPS 2021

26 July 2021

Northern Illinois University

Introduction

$H \to \tau\tau$ is an important Higgs decay channel

- 2nd highest branching ratio among Higgs boson decays to fermions
- The only accessible leptonic decay channel
- Yukawa couplings observed for the first time in $H \to \tau\tau$
- High cross-section (XS) gives access to measuring kinematics of the Higgs boson production and different production modes

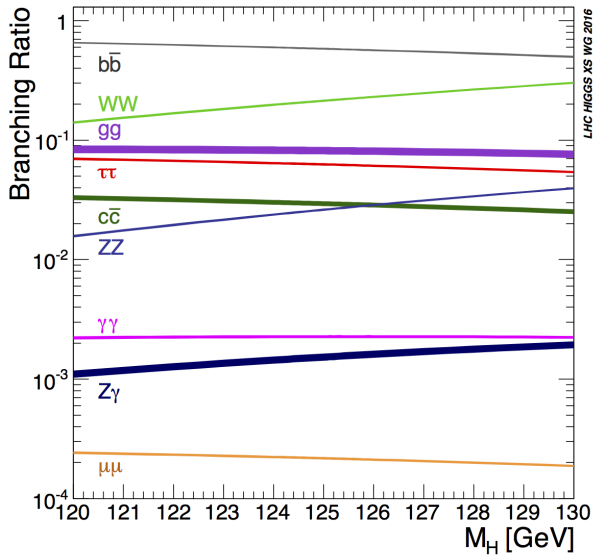

$H \to \tau\tau$ at 125 GeV – History at the LHC

Date	Experiment	Result	Significance Obs. (Exp.) [σ]	Luminosity at 7/8/13 TeV [fb^{-1}]	Reference
May 2014	CMS	evidence	3.2 (3.7)	4.9+19.7	link
April 2015	ATLAS	evidence	4.5 (3.4)	4.5+20.3	link
August 2016	**ATLAS+CMS**	**observation**	5.5 (5.0)	$\sim$ 25	link
April 2018	CMS	observation	5.9 (5.9)	4.9 + 19.7 + 35.9	link
June 2018	**ATLAS**	**observation**	6.4 (5.4)	4.5+20.3+36.1	link
July 2020	CMS	measurements	-	137	link
TODAY	**ATLAS**	**measurements**	-	**139**	link

Scope of the analysis (Full Run-2 dataset)

- Measure $\sigma(H \to \tau\tau)$ as precisely as possible
  - Considering all tau decay combinations: $\tau_{\text{had}}\tau_{\text{had}}$, $\tau_\ell\tau_{\text{had}}$ (where $\ell = e, \mu$), $\tau_e\tau_\mu$
    - The final states with two same-flavour light leptons $\tau_e\tau_e$ and $\tau_\mu\tau_\mu$, not considered due to large uncertainties in $Z \to ee$ and $Z \to \mu\mu$ contributions to the background expectation
  - Sensitive to individual production modes: ggF, VBF, V(had)H and ttH
  - Kinematic properties for ggF: p_{T}(H), N(jets)
  - Cross-section measurements within the Simplified Template Cross-Section (STXS) framework
  - The mass of the di-τ pairs ($m_{\tau\tau}^{\text{MMC}}$) is estimated using the Missing Mass Calculator (MMC) algorithm

- Main analysis improvements/changes with respect to previous results (36.1 fb^{-1}):
  - Object-level embedding to validate $Z \to \tau\tau$+jets predictions and control its normalisation in the signal regions (SRs)
  - Consolidated Misidentified τ (fake) estimate in $\tau_e\tau_\mu$, $\tau_{\text{had}}\tau_{\text{had}}$
  - MVA discriminants to enhance VBF, V(had)H and tt(0L)H$\to\tau_{\text{had}}\tau_{\text{had}}$ production modes
    - V(had)H complementary to V(lep)H analysis
    - New tt(0L)H$\to\tau_{\text{had}}\tau_{\text{had}}$ complementary to ttH multi-lepton analysis
  - Split of the ggH phase space in p_{T}(H)$\times$N(jets) bins

Event selection and categorisation

Event selection

$\tau_e\tau_\mu$	$\tau_e\tau_{\text{had}}/\tau_\mu\tau_{\text{had}}$	$\tau_{\text{had}}\tau_{\text{had}}$
$1e$ and 1μ of opposite sign	$1e/1\mu$ and $1\tau_{\text{had}}$ of opposite sign	$2\tau_{\text{had}}$ of opposite sign
$m_{\tau\tau}^{\text{coll}} > m_Z - 25$ GeV	$m_{\text{T}} < 70$ GeV	$\Delta R_{\tau_{\text{had-vis}}\tau_{\text{had-vis}}} > 0.6$
30 GeV $< m_{e\mu} < 100$ GeV		
veto b-jets	veto b-jets	veto b-jets (except of tt(0L)H$\to\tau_{\text{had}}\tau_{\text{had}}$)
Leading jet $p_{\text{T}} > 40$ GeV	Leading jet $p_{\text{T}} > 40$ GeV	Leading jet $p_{\text{T}} > 70$ GeV, $\lvert\eta\rvert < 2.5$

- Plus additional selection criteria

Event categorisation

VBF inclusive	sub-leading jet $p_{\text{T}} > 30$ GeV $m_{jj} > 350$ GeV, $\lvert\Delta\eta_{jj}\rvert > 3$ $\eta(j_0) \times \eta(j_1) < 0$ lepton centrality: τ visible decay products between VBF jets
VH inclusive	sub-leading jet $p_{\text{T}} > 30$ GeV 60 GeV $< m_{jj} <$ 120 GeV
tt(0L)H$\to\tau_{\text{had}}\tau_{\text{had}}$	# of jets ≥ 6 and # of b-jets ≥ 1 # of jets ≥ 5 and # of b-jets ≥ 2
Boost inclusive	Not VBF, VH, ttH inclusive $p_{\text{T}}(H) > 100$ GeV

Event categorisation

VBF, VH and $t\bar{t}$H events further split with BDT taggers into two categories:

- **VBF tagger**
  - Targeting VBF topology
  - Rejecting ggF and $Z \to \tau\tau$ events
  - VBF_1 (VBF_0) signal purity vs other Higgs production modes is 94% (63%)
- **VH tagger**
  - Targeting VH production mode
  - Rejecting other Higgs production modes
  - Expected fraction of V(had)H among all Higgs boson events is 66% (24%) in VH_1 (VH_0)
- **BDTs for $t\bar{t}$H**
  - Employ two BDTs
  - Reject $Z \to \tau\tau$ and $t\bar{t}$ background
  - $t\bar{t}$H_1 ($t\bar{t}$H_0) signal purity vs other Higgs production modes is 92% (74%)

Boost categorisation based on p_T(H) and $N_{jets}(p_T > 30$ GeV$)$

$N_{jets}(p_T > 30\,\text{GeV})$	$p_T(H)$ bins in GeV [100, 120]	[120, 200]	[200, 300]	[300, ∞[
Exactly 1	boost_0_1J	boost_1_1J	boost_2	boost_3
At least 2	boost_0_ge2J	boost_1_ge2J		

Event categorisation and STXS bins targeted

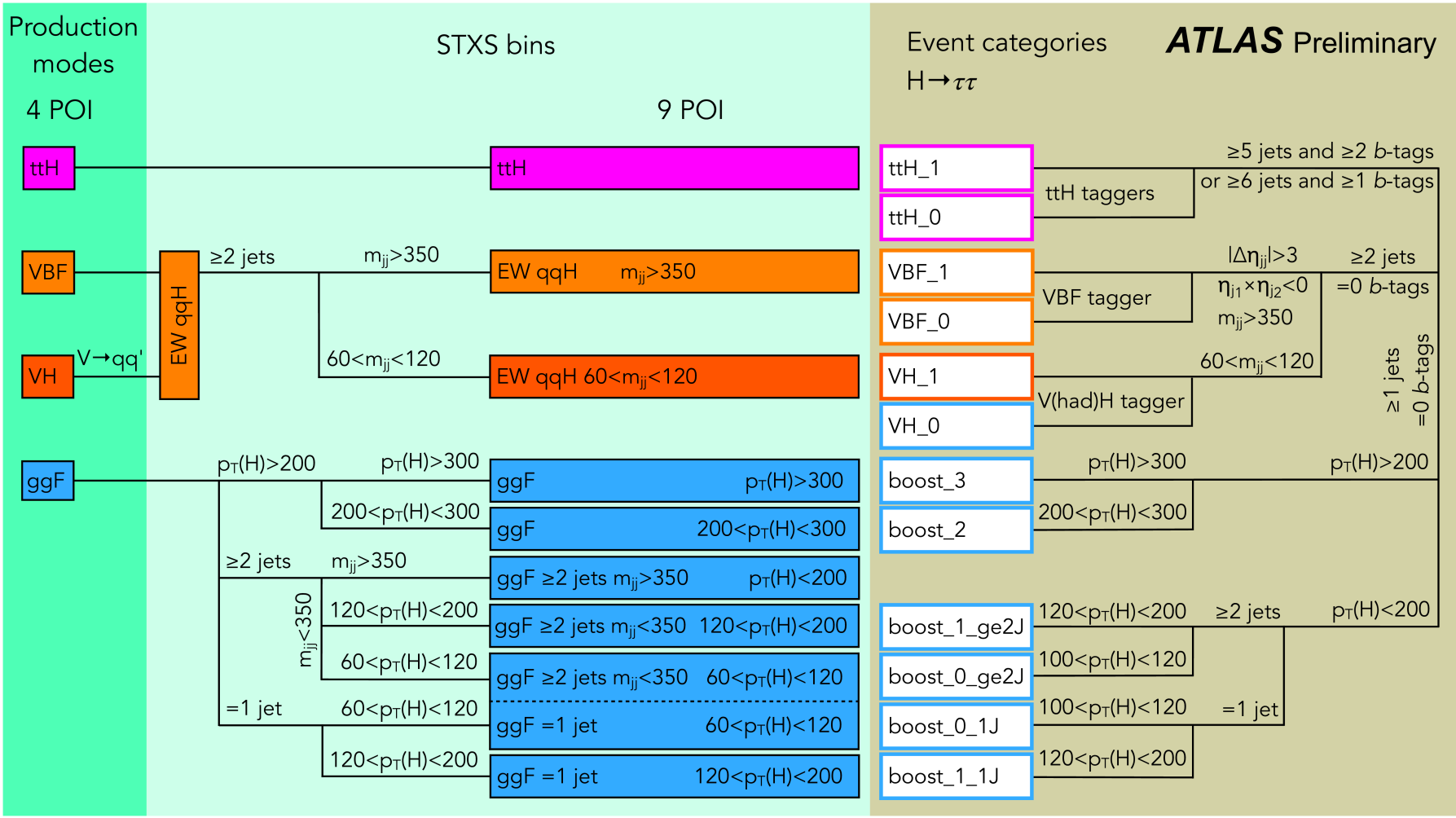

Sketch of the event categorisation and the STXS bins targeted. The dominant STXS bin contributing to each event category is indicated by the colour of the category box or the STXS bin adjacent to it. The background colours on the left side indicate which parameters of interest (POI) are estimated in the fit.

Background estimates

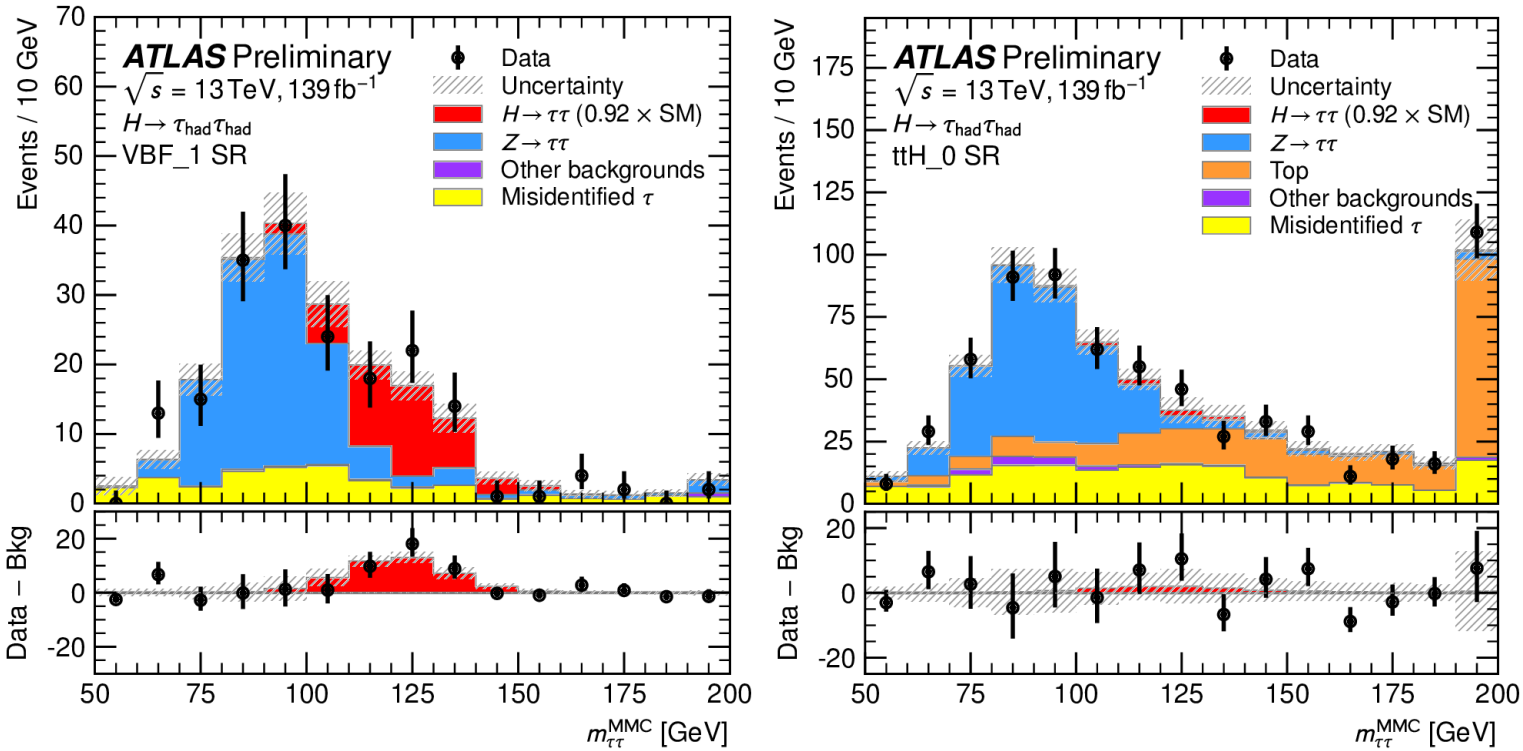

MC-based with data control regions (CRs), except for misidentified τ estimates, which are fully data-driven:

- $Z \to \tau\tau$: **70-90%**: Validated + normalised using embedded $Z \to \ell\ell$ CRs
- **Misidentified τ: 5-20%**: Matrix method ($\tau_e\tau_\mu$), fake factors ($\tau_\ell\tau_{\text{had}}$, $\tau_{\text{had}}\tau_{\text{had}}$)
- **Top: $< 5\%$ ($30 - 35\%$ in $t\bar{t}H$ SRs)**: Validated in Top CR with inverted N(b-jet) criteria
- **Other backgrounds ($Z \to \ell\ell$, $H \to WW$, ...)**: small, taken from MC

$Z \to \tau\tau$ background modelling using $Z \to \ell\ell$ events

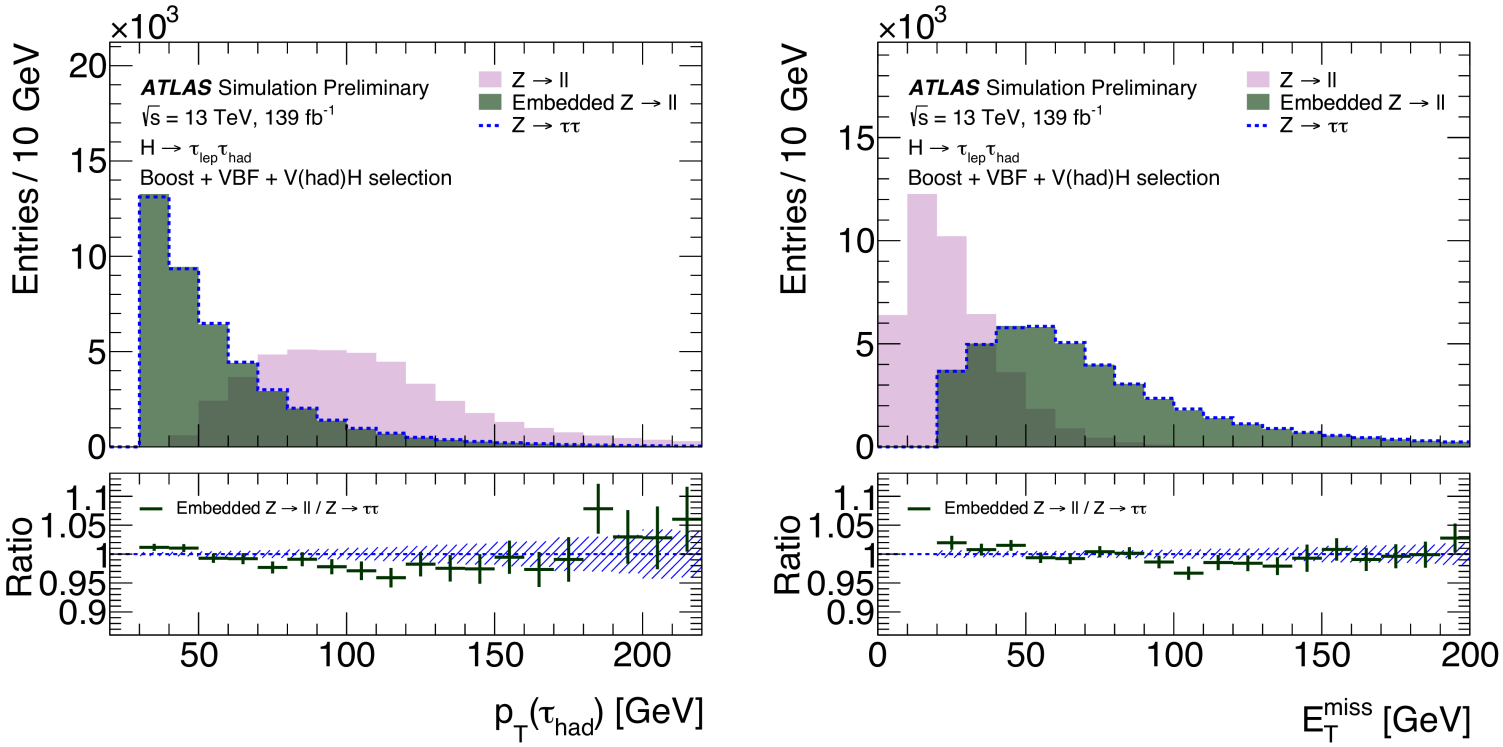

- To mimic the Z boson kinematics and the associated production of jets in $Z(\to \tau\tau)$+jets events, $Z(\to \ell\ell)$+jets events are modified through a simplified embedding procedure
  - The 4-vector of the reconstructed muon (or electron) is replaced by a 4-vector rescaled to parameterise the τ-lepton decay kinematics and energy calibration
  - Validated comparing $Z \to \ell\ell$ simulated events after the embedding, to $Z \to \tau\tau$ simulations
- Used to validate the Z+jets MC modelling and to control the $Z \to \tau\tau$ normalisation in each SR

Fit setup

Fit

- All fits based on the same 32 SRs, differ in how the (parameters of interest) POIs are defined in the likelihood
- 3 types of fit with different number of POIs
  - **1 POI:** inclusive $pp \to H \to \tau\tau$ cross-section
  - **4 POI:** inclusive production mode cross-sections (ggH, VBF, V(had)H, ttH)
  - **9 POIs:** STXS bins
- Di-tau mass estimator $m_{\tau\tau}^{\text{MMC}}$ used as the observable in the SRs
- Single-bin distribution used for the CRs, only normalisation is fitted

Regions

- 32 SRs
  - 10 SRs (boost: 6 SRs, VBF: 2 SRs, VH: 2 SRs) for each final state
  - 2 ttH SRs (only in $\tau_{\text{had}}\tau_{\text{had}}$)
- 30 $Z \to \tau\tau$ CRs
  - One for each SR except ttH SRs
- 6 Top CRs
  - One for each SR in $\tau_\ell\tau_{\text{had}}$ and $\tau_e\tau_\mu$

Results: Total and production mode cross-sections

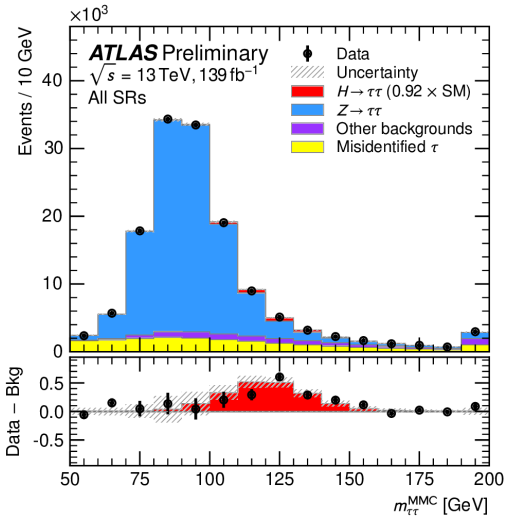

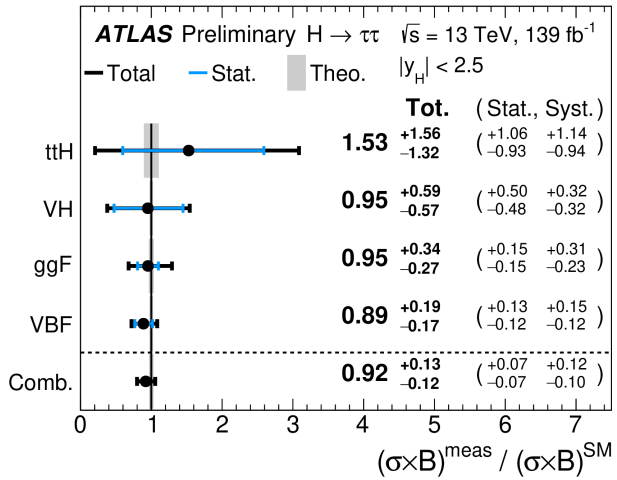

Source of uncertainty	Impact on $\Delta\sigma/\sigma(pp \to H \to \tau\tau)$ [%] Observed	Expected
Theoretical uncertainty in signal	8.1	8.6
Jet and $\vec{E}_{\mathrm{T}}^{\mathrm{miss}}$	4.2	4.1
Background sample size	3.7	3.4
Hadronic τ decays	2.0	2.1
Misidentified τ	1.9	1.8
Luminosity	1.7	1.8
Theoretical uncertainty in Top processes	1.4	1.2
Theoretical uncertainty in Z+jets processes	1.1	1.1
Flavor tagging	0.5	0.5
Electrons and muons	0.4	0.3
Total systematic uncertainty	11.1	11.0
Data sample size	6.6	6.3
Total	12.8	12.5

- $pp \to H \to \tau\tau$ **cross-section measured to be** $2.90 \pm 0.21(\mathrm{stat})^{+0.37}_{-0.32}(\mathrm{syst})$ **pb**
  - In agreement with the SM value of 3.15 ± 0.09 pb
  - Previous ATLAS result using 36.1 fb^{-1} $3.77 \pm 0.60(\mathrm{stat})^{+0.87}_{-0.74}(\mathrm{syst})$ pb

- **Production cross-section measured in the four dominant production modes**
  - All results consistent with the SM predictions
  - Established the **observation of the VBF production** of the $H \to \tau\tau$ with an observed (expected) significance of 5.3σ (6.2σ)
    - $\sigma^{\mathrm{VBF}}_{H\to\tau\tau}$: $0.28 \pm 0.09(\mathrm{stat})^{+0.11}_{-0.09}(\mathrm{syst})$ pb (36.1 fb^{-1}) $\to$ $0.196^{+0.028}_{-0.027}(\mathrm{stat})^{+0.032}_{-0.025}(\mathrm{syst})$ pb
  - The **ggF production** established with an observed (expected) **significance of** 3.9σ (4.6σ)
    - $\sigma^{ggF}_{H\to\tau\tau}$: $3.1 \pm 1.0(\mathrm{stat})^{+1.6}_{-1.3}(\mathrm{syst})$ pb (36.1 fb^{-1}) $\to$ $2.7 \pm 0.4(\mathrm{stat})^{+0.9}_{-0.6}(\mathrm{syst})$ pb

Results: Simplified Template Cross-Section

$pp \to H \to \tau\tau$ XS measured as a function of p_T(H), N_{jets} and invariant mass of two jets (m_{jj})

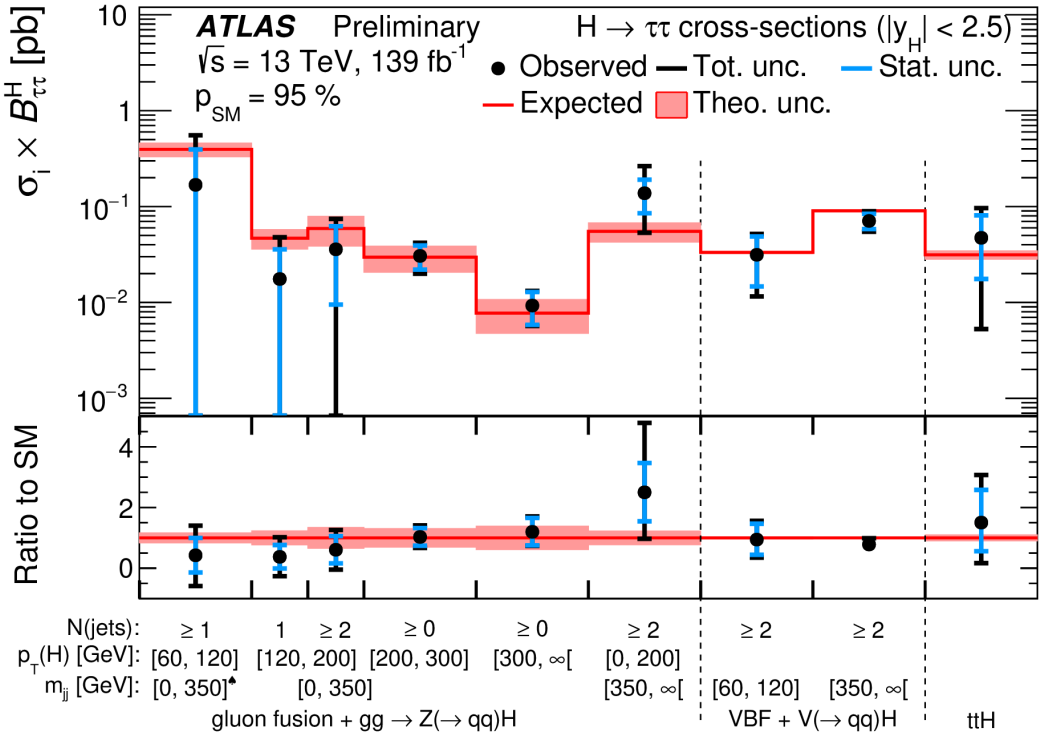

- The results are in agreement with the SM expectations
- The measurements reach precision of **24% for the EW production with $m_{jj} > 350$ GeV**
- The ggF production measured with a precision of 36% and 40% in the p_T(H) interval between 200 GeV and 300 GeV and p_T(H)>300 GeV

Conclusion

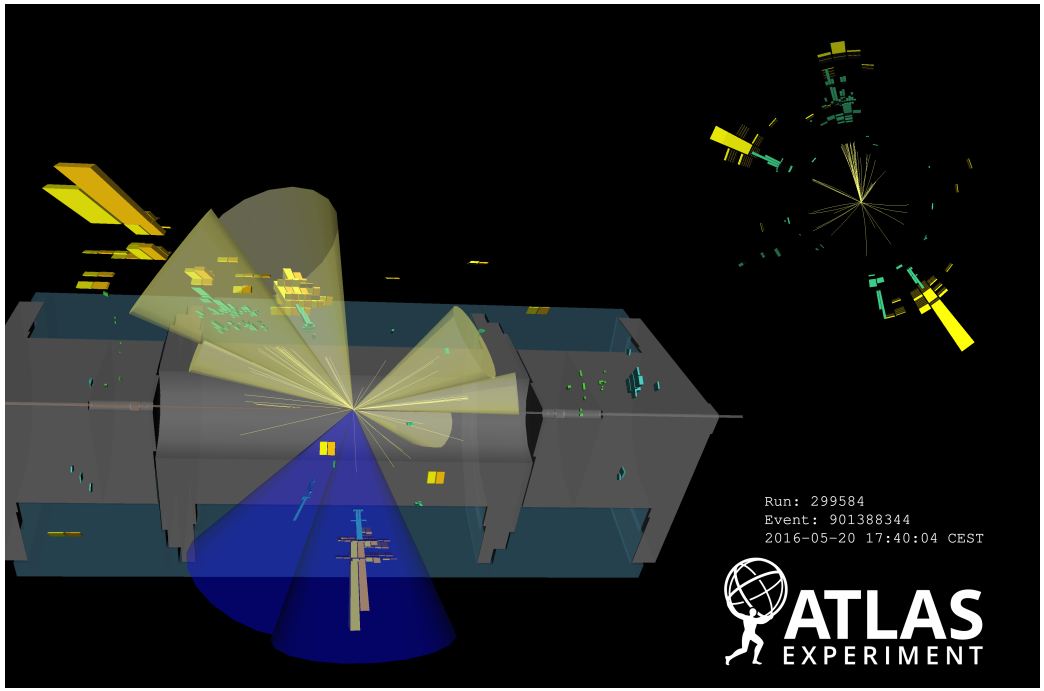

SM $H \to \tau\tau$ measurements using 139 fb^{-1} of data collected by the ATLAS experiment presented

- The total cross-section in the $H \to \tau\tau$ decay channel is measured to be $2.90^{+0.21}_{-0.21}(\text{stat})^{+0.37}_{-0.32}(\text{syst})$
- Total cross-sections determined separately for the four dominant production modes
- Differential measurements using the simplified template cross-section framework performed
- All measurements are in agreement with the SM predictions
- More details in ATLAS-CONF-2021-044

BONUS SLIDES

Previous results

- Last round of the analysis done using 36.1 fb^{-1} of 2015-2016 data

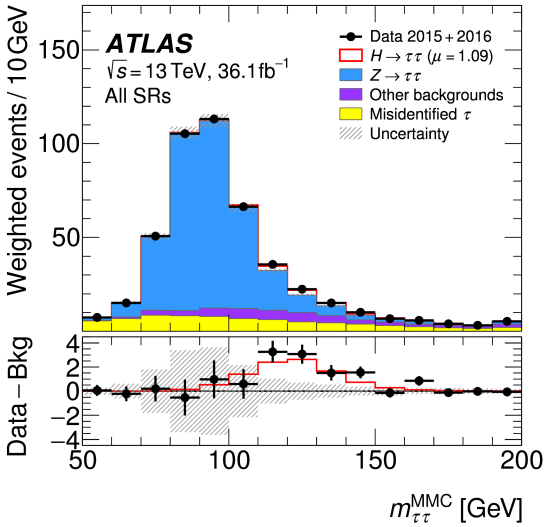

	σ/σ_{SM}	Uncert
Inclusive	**1.09**	±0.35
VBF	**1.18**	±0.51
***gg*H**	**1.02**	±0.62

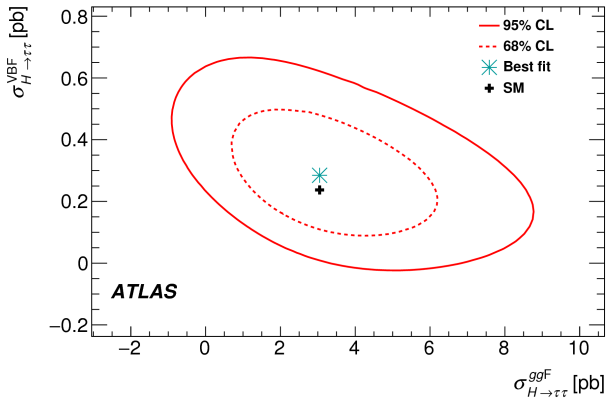

Source of uncertainty	Impact $\Delta\sigma/\sigma_{H\to\tau\tau}$ [%] Observed	Expected
Theoretical uncert. in signal	+13.4 / −8.7	+12.0 / −7.8
Background statistics	+10.8 / −9.9	+10.1 / −9.7
Jets and E_T^{miss}	+11.2 / −9.1	+10.4 / −8.4
Background normalization	+6.3 / −4.4	+6.3 / −4.4
Misidentified τ	+4.5 / −4.2	+3.4 / −3.2
Theoretical uncert. in background	+4.6 / −3.6	+5.0 / −4.0
Hadronic τ decays	+4.4 / −2.9	+5.5 / −4.0
Flavor tagging	+3.4 / −3.4	+3.0 / −2.3
Luminosity	+3.3 / −2.4	+3.1 / −2.2
Electrons and muons	+1.2 / −0.9	+1.1 / −0.8
Total systematic uncert.	+23 / −20	+22 / −19
Data statistics	±16	±15
Total	+28 / −25	+27 / −24

- Measurement of $pp \to H \to \tau\tau$ total cross-section
- Simplified Template Cross-Section (STXS) measurement (not aligned with STXS binning)

Process	Particle-level selection	σ [pb]	σ^{SM} [pb]
*gg*F	$N_{jets} \geq 1$, $60 < p_T^H < 120$ GeV, $\lvert y_H \rvert < 2.5$	$1.79 \pm 0.53(\text{stat.}) \pm 0.74(\text{syst.})$	0.40 ± 0.05
*gg*F	$N_{jets} \geq 1$, $p_T^H > 120$ GeV, $\lvert y_H \rvert < 2.5$	$0.12 \pm 0.05(\text{stat.}) \pm 0.05(\text{syst.})$	0.14 ± 0.03
VBF	$\lvert y_H \rvert < 2.5$	$0.25 \pm 0.08(\text{stat.}) \pm 0.08(\text{syst.})$	0.22 ± 0.01

- Good agreement with the Standard Model (SM) prediction
- Limited by: uncertainty on *gg*H predictions, background statistics, jet uncertainties

Event selection

	$\tau_e\tau_\mu$	$\tau_{\text{lep}}\tau_{\text{had}}$		$\tau_{\text{had}}\tau_{\text{had}}$
		$\tau_e\tau_{\text{had}}$	$\tau_\mu\tau_{\text{had}}$	
N(e)	1	1	0	0
N(μ)	1	0	1	0
N($\tau_{\text{had-vis}}$)	0	1	1	2
e p_{T} cut [GeV]	27, 15, 18	27		
μ p_{T} cut [GeV]	10, 27.3, 14.7		27.3	
$\tau_{\text{had-vis}}$ p_{T} cut [GeV]		30		40, 30
Identification	e/μ: Medium	$e/\mu/\tau_{\text{had-vis}}$: Medium		$\tau_{\text{had-vis}}$: Medium
Isolation	e: Loose μ: Tight	e: Loose	μ: Tight	
Charge	Opposite charge	Opposite charge		Opposite charge
Kinematics	$m_{\tau\tau}^{\text{coll}} > m_Z - 25\,\text{GeV}$ $30\,\text{GeV} < m_{e\mu} < 100\,\text{GeV}$	$m_{\text{T}} < 70\,\text{GeV}$		
b-veto	# of b-jets = 0	# of b-jets = 0		# of b-jets = 0 (≥ 1 or 2 in ttH categories)
$E_{\text{T}}^{\text{miss}}$	$E_{\text{T}}^{\text{miss}} > 20\,\text{GeV}$	$E_{\text{T}}^{\text{miss}} > 20\,\text{GeV}$		$E_{\text{T}}^{\text{miss}} > 20\,\text{GeV}$
Leading jet	$p_{\text{T}} > 40\,\text{GeV}$	$p_{\text{T}} > 40\,\text{GeV}$		$p_{\text{T}} > 70\,\text{GeV}$, $\lvert\eta\rvert < 3.2$
Angular	$\Delta R_{e\mu} < 2.0$ $\lvert\Delta\eta_{e\mu}\rvert < 1.5$	$\Delta R_{\ell\tau_{\text{had-vis}}} < 2.5$ $\lvert\Delta\eta_{\ell\tau_{\text{had-vis}}}\rvert < 1.5$		$0.6 < \Delta R_{\tau_{\text{had-vis}}\tau_{\text{had-vis}}} < 2.5$ $\lvert\Delta\eta_{\tau_{\text{had-vis}}\tau_{\text{had-vis}}}\rvert < 1.5$
Coll. app. x_1/x_2	$0.1 < x_1 < 1.0$ $0.1 < x_2 < 1.0$	$0.1 < x_1 < 1.4$ $0.1 < x_2 < 1.2$		$0.1 < x_1 < 1.4$ $0.1 < x_2 < 1.4$

Event categorisation

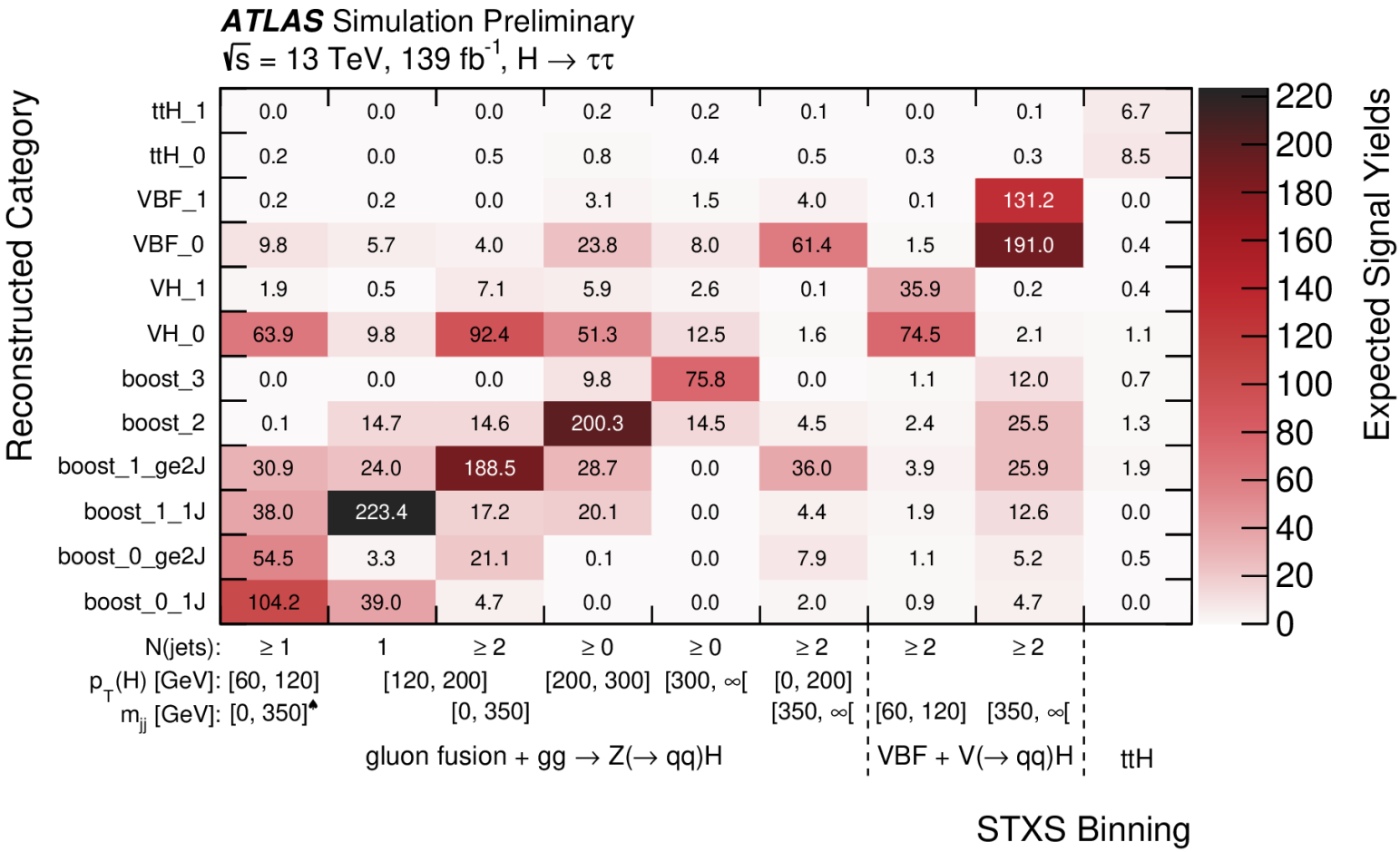

Expected $H \to \tau\tau$ signal yield in each of the reconstructed event category of the analysis (y-axis) for each of the nine measured STXS bins (x-axis).

Event categorisation

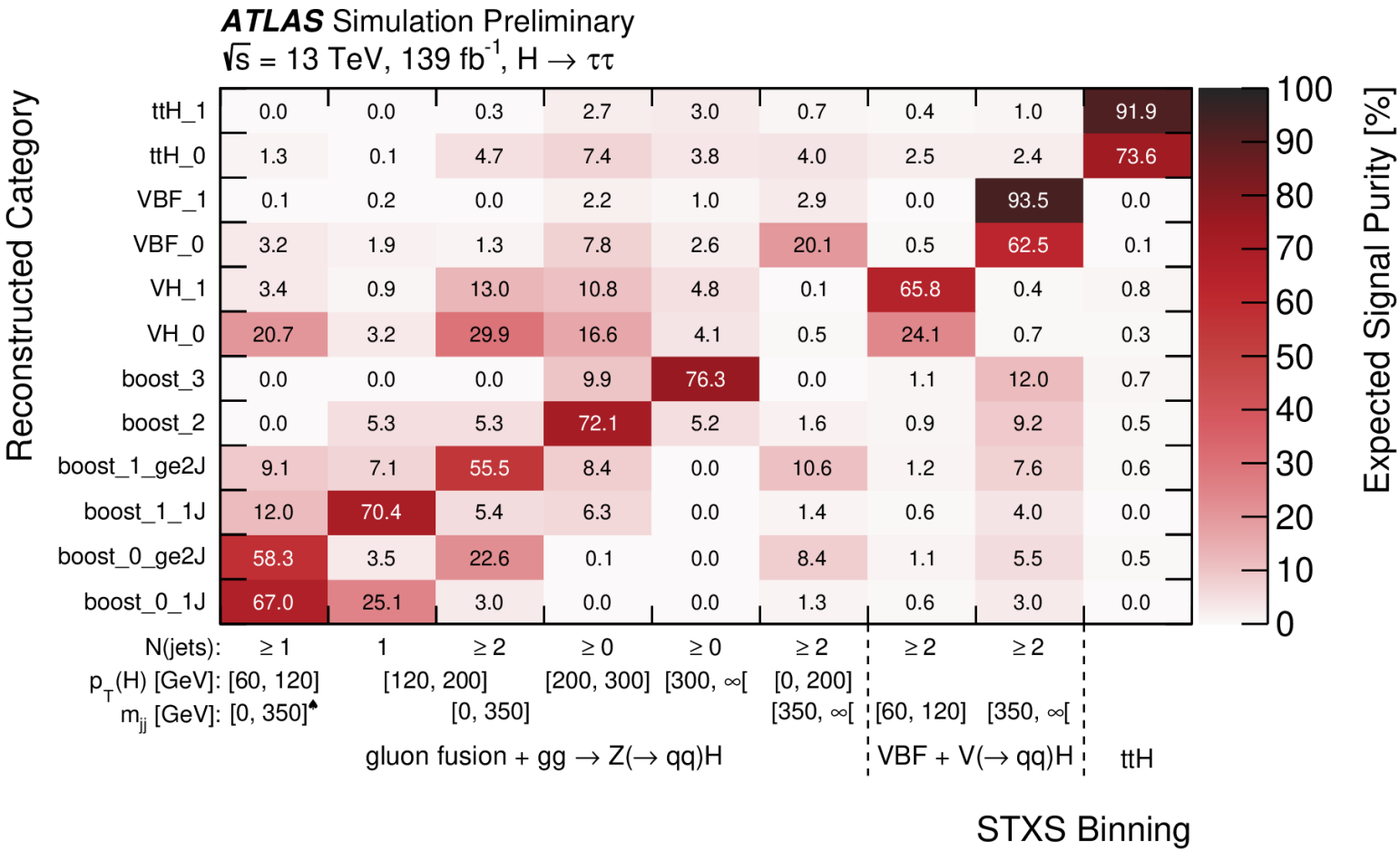

Relative contribution of each of the nine measured STXS bins to the total $H \to \tau\tau$ signal expectation in each reconstructed event category. Yields are summed over the three decay channels.

Multivariate taggers

	Variable	VBF	V(had)H	ttH vs $t\bar{t}$	ttH vs $Z \to \tau\tau$
Jet properties	Invariant mass of 2 leading jets	•	•		
	$p_{\mathrm{T}}(jj)$	•	•		
	Product of η of 2 leading jets	•			
	Sub-leading jet p_{T}	•			
	Leading jet η				•
	Sub-leading jet η				•
	Scalar sum of all jets p_{T}			•	•
	Scalar sum of all b-tagged jets p_{T}				•
	Best W-candidate dijet invariant mass			•	•
	Best t-quark-candidate three-jet invariant mass			•	•
Angular distances	$\Delta\phi$(jet 0, jet 1)	•			
	$\lvert\Delta\eta$(jet 0, jet 1)$\rvert$	•	•		
	ΔR(jet 0, jet 1)		•		
	$\Delta R(\tau\tau, jj)$		•		
	$\Delta R(\tau, \tau)$		•	•	
	Smallest ΔR (any 2 jets)			•	
	$\lvert\Delta\eta(\tau, \tau)\rvert$			•	•
τ prop.	$p_{\mathrm{T}}(\tau\tau)$			•	
	Sub-leading τ p_{T}				•
	Sub-leading τ η				•
H cand.	$p_{\mathrm{T}}(Hjj)$	•	•		
	$p_{\mathrm{T}}(H)/p_{\mathrm{T}}(jj)$		•		
$\vec{E}_{\mathrm{T}}^{\mathrm{miss}}$	Missing transverse energy $E_{\mathrm{T}}^{\mathrm{miss}}$		•	•	•
	Smallest $\Delta\phi$ $(\tau, \vec{E}_{\mathrm{T}}^{\mathrm{miss}})$				•

For each tagger, the presence of a bullet indicates whether the variable is used or not.

Background composition

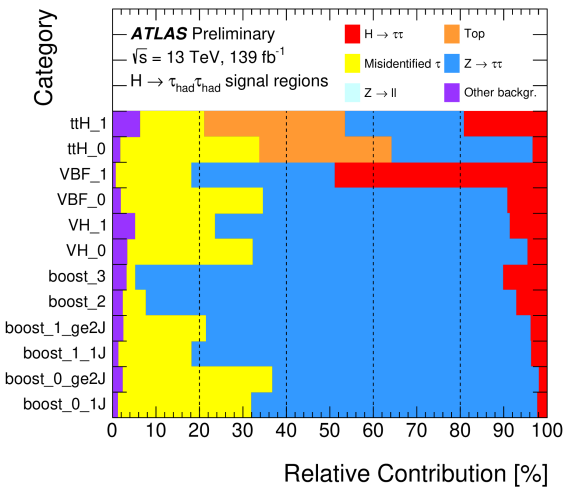

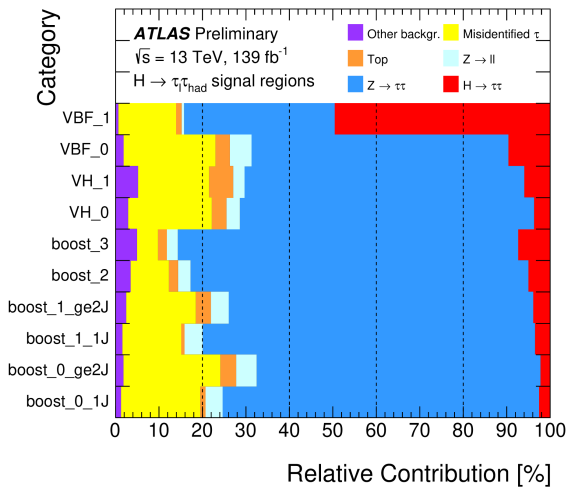

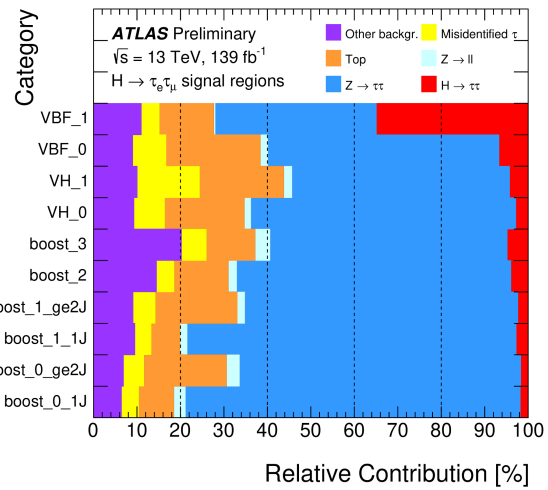

Relative contribution of each process to the total measured yields in each category of the analysis for (left) $\tau_{\text{had}}\tau_{\text{had}}$, (middle) $\tau_\ell\tau_{\text{had}}$ and (right) $\tau_e\tau_\mu$ channels, within $100 < m_{\tau\tau}^{\text{MMC}} < 150$ GeV. 'Other backgrounds' include diboson, $t\bar{t} + V$ and $H \to WW^*$.

$Z \to \tau\tau$ background estimate

Procedure:

1. Select $Z \to \ell\ell$ events
2. Unfold ℓ reconstruction, identification and isolation effects
3. Scale p_ℓ by pasteurisation τ decay effects (scaling term samples from visible reco p_T/total truth p_T distribution)
4. Reweight to account for efficiencies

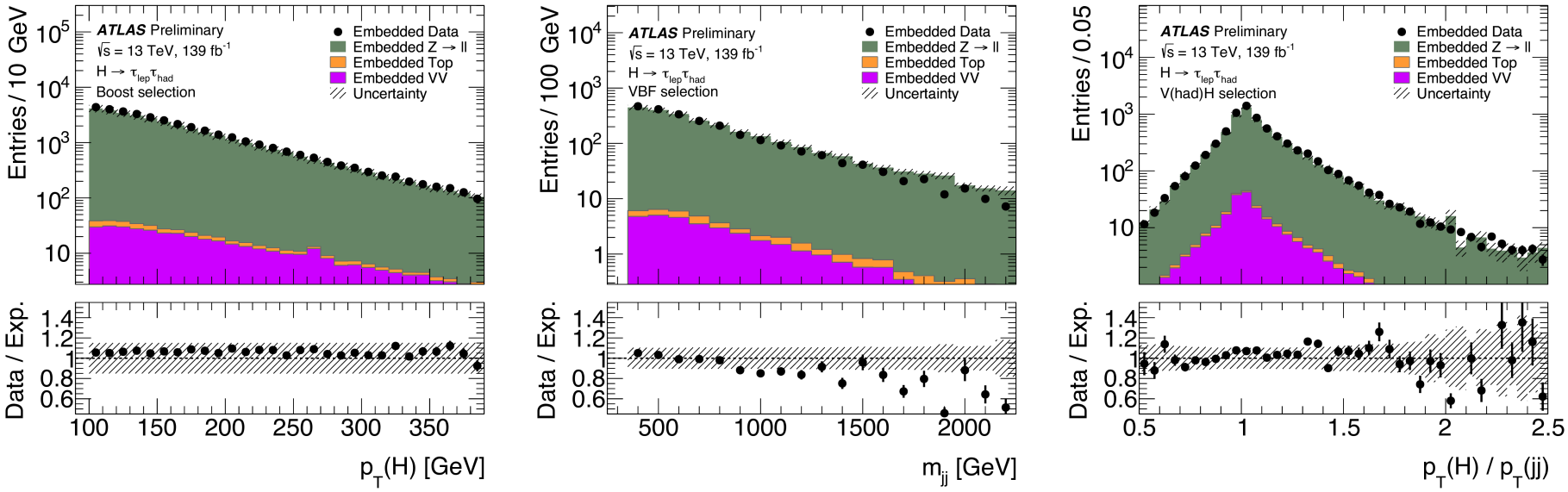

Comparison of MC simulation prediction with data after the embedding procedure is applied to mimic the $\tau_\ell\tau_{\text{had}}$ event selection. The bottom panels represent the agreement between the embedded data and the embedded simulation samples.

Data-driven estimate of Misidentified τ

- Processes with at least one jet mis-identified as an electron, muon or τ_{had} are referred to as Misidentified τ background
- Data events selected using the same criteria as for the SRs with the exception of the criteria that are loosened or inverted
  - electron or muon identification and isolation requirements
  - $\tau_{\text{had-vis}}$ identification criteria
- Transfer factors computed in dedicated control regions and used to correct for kinematic and normalisation differences between the events with altered isolation or identification criteria and the SRs

Data-driven estimate of Misidentified τ

- $\tau_e\tau_\mu$: Matrix method used to determine contributions from **electron fakes** and **muon fakes**
- $\tau_\ell\tau_{\text{had}}$: Fake and isolation factors used, considering τ_{had} fakes as well as τ_{had} + **light lepton fakes**
- $\tau_{\text{had}}\tau_{\text{had}}$: Fake factors used to determine contributions from **single** and **double** tau fakes (mainly from QCD)

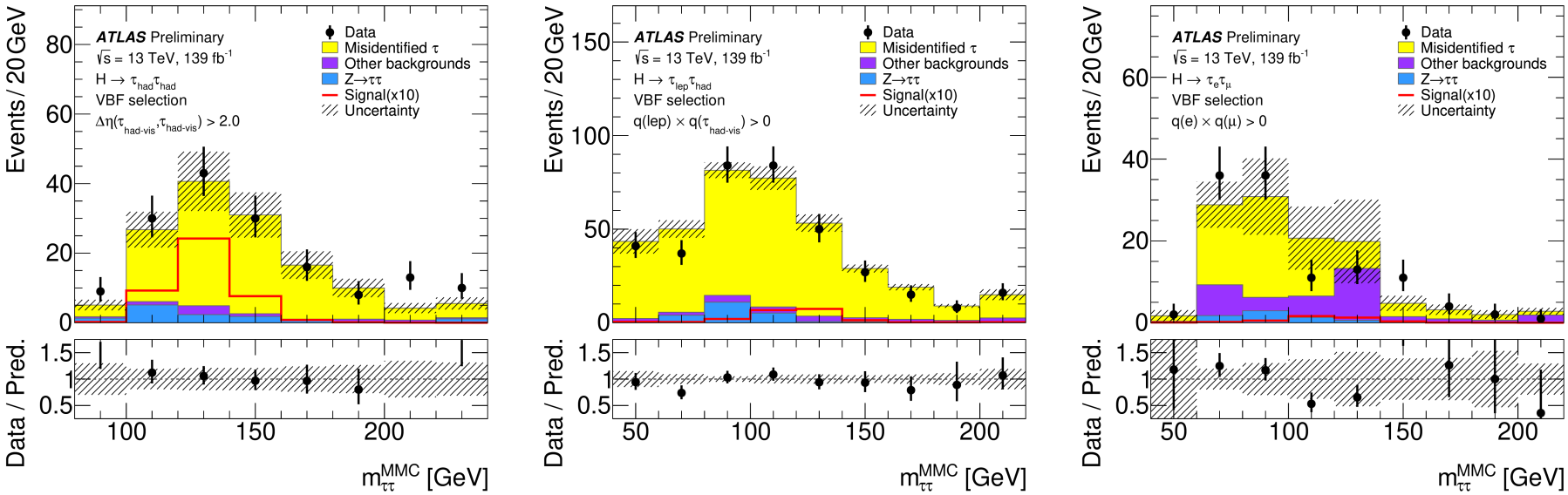

Validation of the data-driven estimate of the processes (left) with jets misidentified as $\tau_{\text{had-vis}}$ in $\tau_{\text{had}}\tau_{\text{had}}$ final state, (middle) with light leptons and $\tau_{\text{had-vis}}$ of the same charge in the τ_ℓ τ_{had} channel, and (right) with jets misidentified as electrons or muons in τ_e,τ_μ events with same charge leptons. The hashed band represents the statistical uncertainty due to limited sample sizes and the systematic uncertainty of the data-driven estimate.

Impact on the 1-POI measurement

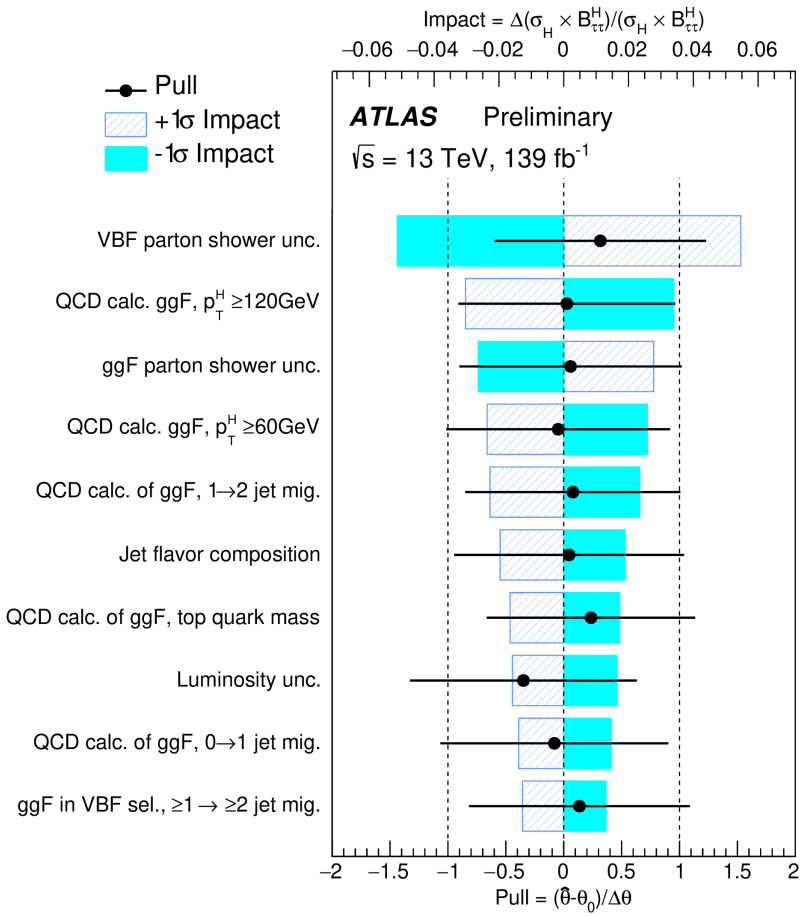

Fractional impact of nuisance parameters in the $pp \to H \to \tau\tau$ cross-section measurement. The ten nuisance parameters with the largest impact are shown in decreasing order. For each nuisance parameter, the dashed (light blue) band shows the fractional impact of a change of one positive (negative) standard deviation. The deviation of each nuisance parameter from their original value is indicated by the black dot and the additional constraint provided by the statistical analysis by the black line.

Fit setup

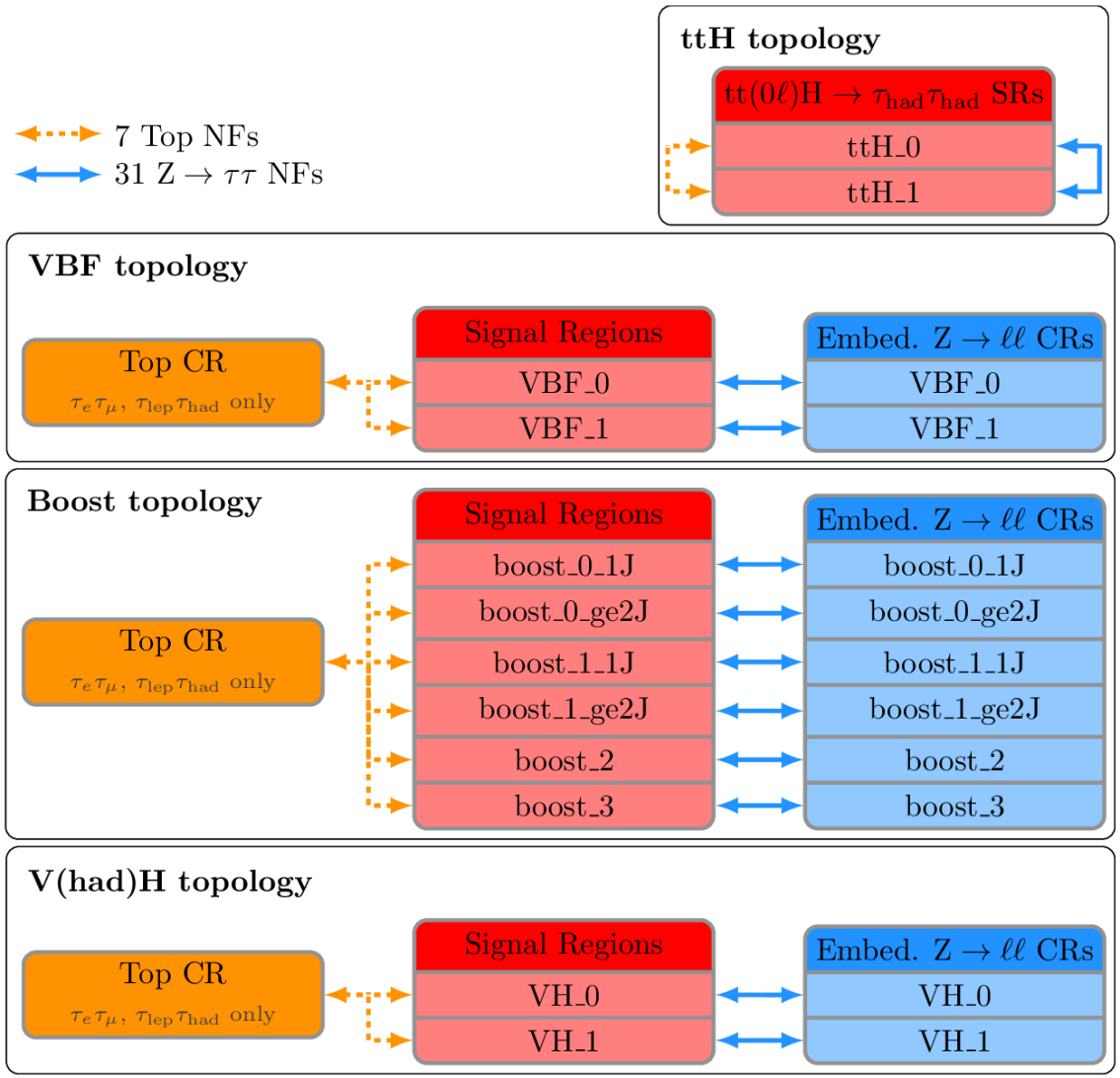

Graphical representation of the regions considered in the likelihood function and the normalisation factors (NFs) defined in the analysis.

Results

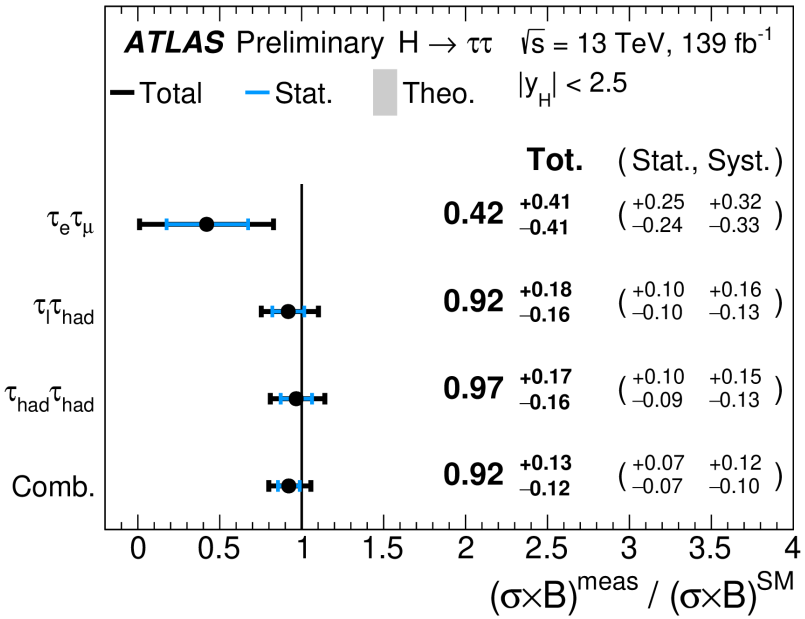

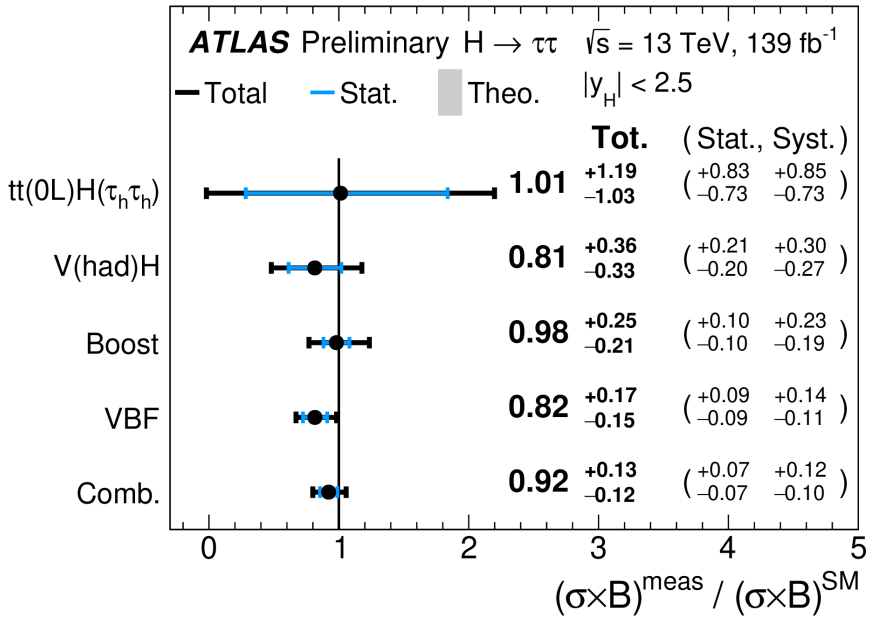

The measured values for $\sigma_H \times \mathcal{B}(H \to \tau\tau)$ relative to the SM expectations when only the data of (left) individual channels or (right) individual categories are used. The total $\pm 1\sigma$ uncertainty in the measurement is indicated by the black error bars, with the individual contribution from the statistical uncertainty in blue.

CMS Results

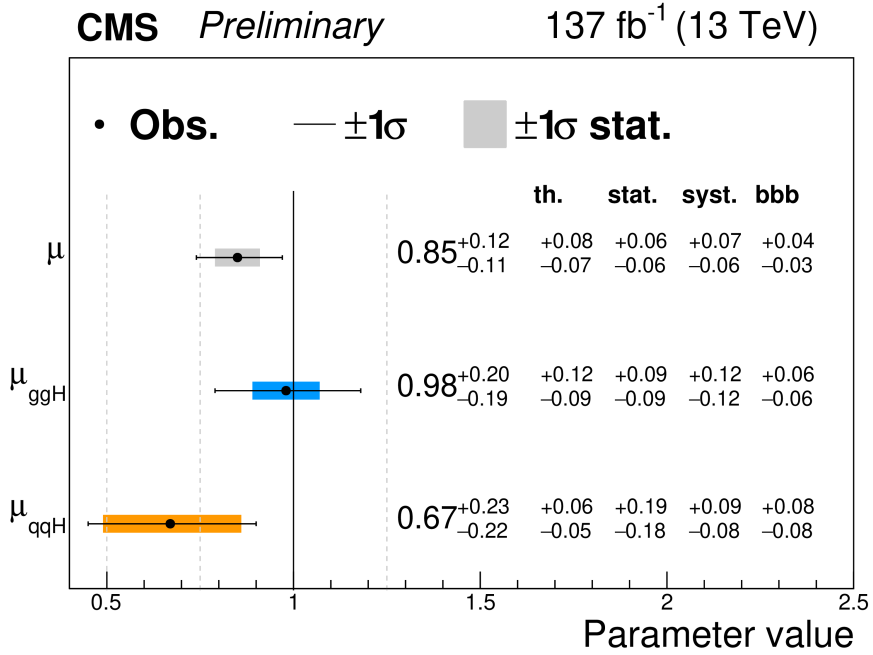

HIG-19-010

Results: 4 POI

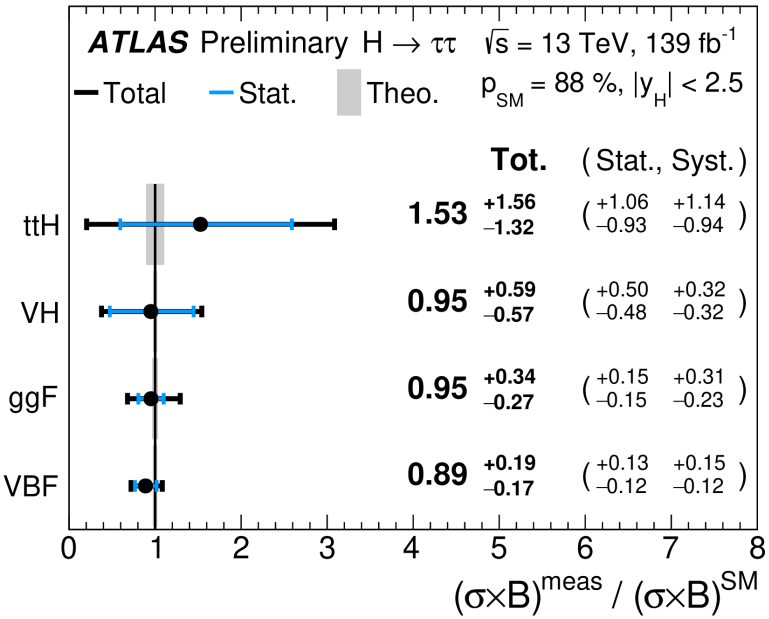

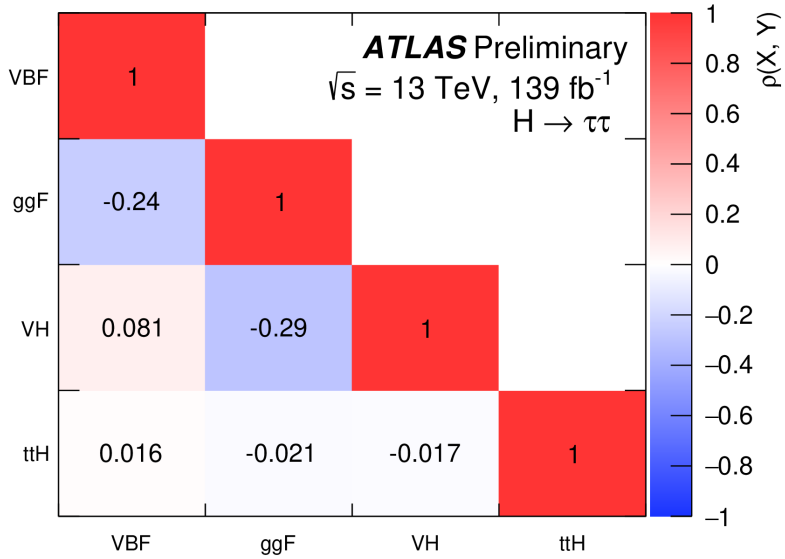

The measured values for $\sigma_H \times \mathcal{B}(H \to \tau\tau)$ relative to the SM expectations when only the data of (left) individual production modes. (right) The measured correlations between each parameter of interest in the measurement of the cross-sections per production mode.

Uncertainties: 4 POI

Production Mode	SM prediction [pb]	Result [pb]	Stat. unc. [pb]	Syst. unc. [pb]		
				Th. sig.	Th. bkg.	Exp.
$t\bar{t}H$	0.031 ± 0.003	0.048 ± 0.045	± 0.027	± 0.011	± 0.027	± 0.018
VH	0.118 ± 0.003	0.11 ± 0.04	± 0.02	± 0.02	± 0.01	± 0.02
ggF	2.8 ± 0.1	2.7 ± 0.9	± 0.4	± 0.6	± 0.1	± 0.5
VBF	0.22 ± 0.01	0.196 ± 0.040	± 0.026	± 0.024	± 0.005	± 0.016
$pp \to H$	3.15 ± 0.09	2.90 ± 0.40	± 0.22	± 0.26	± 0.06	± 0.22

Best-fit values and uncertainties for the total $pp \to H \to \tau\tau$ cross-section and the measurement in the four dominant production modes. The SM predictions for each region, computed using the inclusive cross-section calculations and the simulated event samples are also shown. The contributions to the total uncertainty in the measurements from statistical (Stat. unc.) or systematic uncertainties (Syst. unc.) in the signal prediction (Th. sig.), background prediction (Th. bkg.), and in experimental performance (Exp.) are given separately.

Results: 9 POI

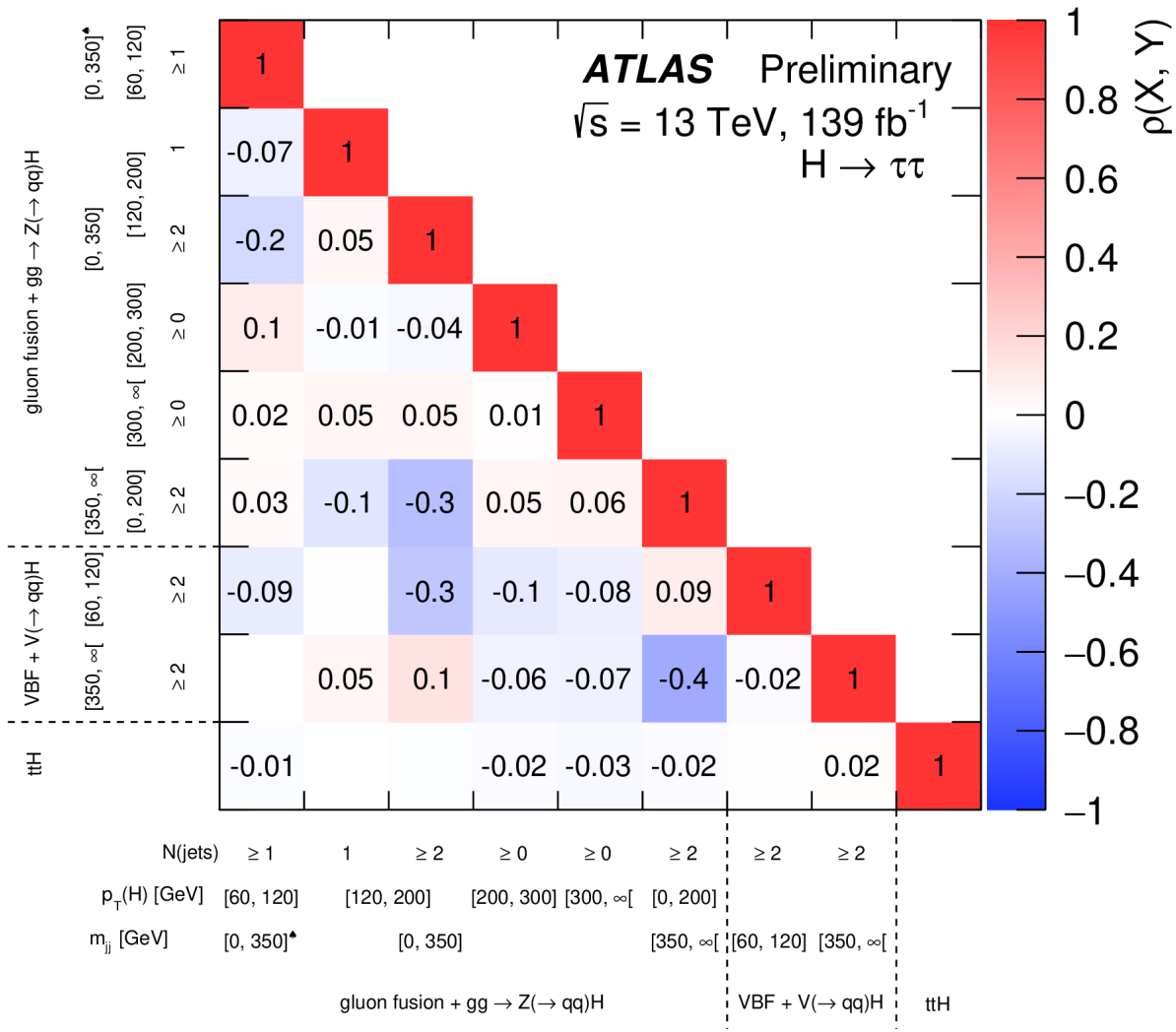

The measured correlations between each pair parameter of interest in the STXS measurement (the criterion on m_{jj} only applies to events with at least two reconstructed jets).

Uncertainties: 9 POI

STXS bin				SM prediction	Result	Stat. unc.	Syst. unc. [pb]		
Process	m_{jj} [GeV]	$p_{\mathrm{T}}(H)$ [GeV]	$\mathrm{N_{jets}}$	[pb]	[pb]	[pb]	Th. sig.	Th. bkg.	Exp.
ggF + $gg \to Z(\to bb)H$	[0, 350]♠	[60, 120]	≥ 1	0.39 ± 0.06	0.17 ± 0.39	± 0.22	± 0.06	± 0.15	± 0.29
		[120, 200]	$= 1$	0.047 ± 0.011	0.018 ± 0.030	± 0.018	± 0.004	± 0.004	± 0.019
	[0, 350]	[120, 200]	≥ 2	0.059 ± 0.020	0.036 ± 0.039	± 0.027	± 0.009	± 0.009	± 0.025
		[200, 300]	≥ 0	0.030 ± 0.009	0.031 ± 0.011	± 0.009	± 0.003	± 0.001	± 0.006
		[300, ∞[	≥ 0	0.008 ± 0.003	0.009 ± 0.004	± 0.003	± 0.001	± 0.000	± 0.001
	[350, ∞[	[0, 200]	≥ 2	0.055 ± 0.013	0.14 ± 0.11	± 0.05	± 0.06	± 0.01	± 0.07
EWK	[60, 120]		≥ 2	0.033 ± 0.001	0.031 ± 0.020	± 0.017	± 0.003	± 0.001	± 0.010
	[350, ∞[		≥ 2	0.090 ± 0.002	0.071 ± 0.017	± 0.014	± 0.010	± 0.002	± 0.006
$t\bar{t}H$				0.031 ± 0.003	0.047 ± 0.046	± 0.032	± 0.011	± 0.027	± 0.018

Best-fit values and uncertainties for the $H \to \tau\tau$ cross-section in the reduced stage 1.2 STXS scheme. The SM predictions for each region, computed using the inclusive cross-section calculations and the simulated event samples are also shown. The EWK production mode includes vector-boson-fusion and $qq \to V(\to qq)H$ processes. The contributions to the total uncertainty in the measurements from statistical (Stat. unc.) or systematic uncertainties (Syst. unc.) in the signal prediction (Th. sig.), background prediction (Th. bkg.), and in experimental performance (Exp.) are given separately.